



Article

Temperature and Density Conditions for Alpha Clustering in Excited Self-Conjugate Nuclei

Bernard Borderie ^{1,*}, Adriana Raduta ², Enrico De Filippo ³ , Elena Geraci ^{3,4}, Nicolas Le Neindre ⁵, Giuseppe Cardella ³, Gaetano Lanzalone ^{6,7}, Ivano Lombardo ³, Olivier Lopez ⁵, Concettina Maiolino ⁶, Angelo Pagano ³ , Massimo Papa ³, Sara Pirrone ³, Francesca Rizzo ^{4,6}  and Paolo Russotto ⁶

¹ CNRS/IN2P3, IJCLab, Université Paris-Saclay, 91405 Orsay, France

² National Institute for Physics and Nuclear Engineering (IFIN-HH), 077125 Bucharest, Romania; araduta@nipne.ro

³ INFN, Sezione di Catania, 95125 Catania, Italy; defilippo@ct.infn.it (E.D.F.); elena.geraci@dfa.unict.it (E.G.); giuseppe.cardella@ct.infn.it (G.C.); ivano.lombardo@ct.infn.it (I.L.); angelo.pagano@ct.infn.it (A.P.); massimo.papa@ct.infn.it (M.P.); sara.pirrone@ct.infn.it (S.P.)

⁴ Dipartimento di Fisica e Astronomia “Ettore Majorana”, Università di Catania, 95123 Catania, Italy; rizzo@lns.infn.it

⁵ ENSICAEN, UNICAEN, CNRS/IN2P3, LPC, Normandie University, 14050 Caen, France; leneindre@lpccaen.in2p3.fr (N.L.N.); lopez@lpccaen.in2p3.fr (O.L.)

⁶ INFN, Laboratori Nazionali del Sud, 95125 Catania, Italy; lanzalone@lns.infn.it (G.L.); cettina.maiolino@lns.infn.it (C.M.); russotto@lns.infn.it (P.R.)

⁷ Facoltà di Ingegneria e Architettura, Università Kore, 94100 Enna, Italy

* Correspondence: bernard.borderie@ijclab.in2p3.fr



Citation: Borderie, B.; Raduta, A.; De Filippo, E.; Geraci, E.; Le Neindre, N.; Cardella, G.; Lanzalone, G.; Lombardo, I.; Lopez, O.; Maiolino, C.; et al. Temperature and Density Conditions for Alpha Clustering in Excited Self-Conjugate Nuclei. *Symmetry* **2021**, *13*, 1562. <https://doi.org/10.3390/sym13091562>

Academic Editors: Stefan Typel, Helena Sofia Pais, Francesca Gulminelli and Yugang Ma

Received: 25 May 2021

Accepted: 17 August 2021

Published: 25 August 2021

Publisher's Note: MDPI stays neutral with regard to jurisdictional claims in published maps and institutional affiliations.



Copyright: © 2021 by the authors. Licensee MDPI, Basel, Switzerland. This article is an open access article distributed under the terms and conditions of the Creative Commons Attribution (CC BY) license (<https://creativecommons.org/licenses/by/4.0/>).

Abstract: Starting from experimental studies on alpha-clustering in excited self-conjugate nuclei (from ^{16}O to ^{28}Si), temperature and density conditions for such a clustering are determined. Measured temperatures have been found in the range of 5.5–6.0 MeV, whereas density values of 0.3–0.4 times the saturation density are deduced, i.e., 0.046 to 0.062 fm $^{-3}$. Such a density domain is also predicted by constrained self-consistent mean field calculations. These results constitute a benchmark for alpha clustering from self-conjugate nuclei in relation to descriptions of stellar evolution and supernovae.

Keywords: alpha-particle clustering; self-conjugate nuclei; temperature; density

1. Introduction

The knowledge of the composition of warm nuclear matter at low density is of paramount importance for a better understanding of the description of the core-collapse of supernovae as well as for the formation and static properties of proto-neutron stars [1,2]. In this context, cluster formation is one of the fundamental aspects with, in particular, the role of α -particles, which are predicted to be present due to the instability of nuclear matter against cluster formation [3–7]. Related to this, the formation of α -particle clustering from excited expanding self-conjugate nuclei was also revealed in two different constrained self-consistent mean field calculations [8–10]. On the experimental side, cluster formation and their in-medium effects have been probed by heavy-ion experiments [11–14] and alpha-clustering was observed in excited expanding self-conjugate nuclei [15–17]. The aim of the present paper is to give a benchmark for the temperature and density needed to observe alpha-clustering in self-conjugate nuclei. The information is derived from experimental data (temperature, freeze-out volume/density) and densities compared with theoretical expectations. The paper is organized as follows. In Section 2, the experimental context and the event selection will be presented. Section 3 is dedicated to alpha-particle clustering (evidence and deduced temperature-density information). Finally, in Section 3, density information from the theoretical side is discussed.

2. Experiment and Event Selection

The experiment was performed at INFN, Laboratori Nazionali del Sud in Catania, Italy. The chosen experimental strategy was to use the reaction $^{40}\text{Ca} + ^{12}\text{C}$ at an incident energy (25 MeV per nucleon) high enough to produce some hot expanding fragmentation products [18,19] associated to a high granularity large solid angle particle array to precisely reconstruct the directions of the velocity vectors. The beam impinging on a thin carbon target ($320\text{ }\mu\text{g}/\text{cm}^2$) was delivered by the Superconducting Cyclotron, and the charged reaction products were detected by the CHIMERA 4π multi-detector [20]. The beam intensity was kept around 10^7 ions/s to avoid pile-up events and random coincidences, which is mandatory for high multiplicity studies. CHIMERA consists of 1192 telescopes (ΔE silicon detectors 200–300 μm thick and CsI(Tl) stopping detectors) mounted on 35 rings that cover 94% of the solid angle with very high granularity at forward angles. Details on A and Z identifications and on the quality of energy calibrations can be found in Refs. [15,20–22]. One can just underline that careful identifications and selections were allowed by a complete exclusive detection in A and Z of all reaction products and by the excellent forward granularity of CHIMERA; energy resolution was better than 1% for silicon detectors and varies between 1.0% and 2.5% for alpha particles stopped in CsI(Tl) crystals.

As a first step in our event selection procedure, we want to exclude poorly-measured events. Without making any hypothesis about the physics of the studied reaction, one can measure the total detected charge Z_{tot} (neutrons are not measured). Due to their cross-sections and the geometrical efficiency of CHIMERA, the well-detected reaction products correspond to projectile fragmentation (PF) [18,19] with $Z_{tot} = 19$ –20 (target reaction products not detected) and to incomplete/complete fusion with $Z_{tot} = 21$ –26 [23]. At this stage, we can have the first indication of the multiplicity of α -particles, M_α , emitted per event for well-identified mechanisms ($Z_{tot} \geq 19$ —see Figure 1 from Ref. [15]). M_α extends up to thirteen, which means a deexcitation of the total system into α -particles. Moreover, a reasonable number of events exhibit M_α values up to about 6–7.

The goal is now to tentatively isolate, in the detected events, reaction products emitting α -particles only. Refs. [19,24] have shown that, at incident energies close to ours, ^{20}Ne or ^{32}S PF is dominated by alpha-conjugate reaction products. Based on this, and expecting the same for ^{40}Ca , we restrict our selection to completely detected PF events ($Z_{tot} = 20$) composed of one projectile fragment and α -particles. Charge conservation imposes $Z_{frag} = 20 - 2M_\alpha$. An example of the mass distribution of the single fragment can be seen in Ref. [15].

After this double selection, the question is: from which emission source are the α -particles emitted? Several possibilities are present, and further selections must be made before restricting our study to alpha-sources emitting exclusively the M_α observed (called $N\alpha$ sources in what follows). Possibilities that we must examine are the following:

(I) Considering the incident energy of the reaction and the forward focusing of reaction products, it is important to identify the possible presence of preequilibrium (PE) α -particles in our selected PF events. With the hypothesis that all the α -particles are emitted from their center-of-mass reference frame, we noted an energy distribution that resembles a thermal one with the presence of a high energy tail starting at 40 MeV, which signs PE emission (see Figure 3 from Ref. [15]). To prevent errors on alpha emitter properties, it is necessary to remove events in which such PE emission can be present; an upper energy limit of 40 MeV found irrespective of M_α was imposed to the α -particle energy. At this stage, 6.9% to 9.2% of events were excluded.

(II) α -particles can be emitted from the de-excitation of PF events via unbound states of ^{12}C , ^{16}O , ^{20}Ne and not directly from excited expanding $N\alpha$ sources. We want, for instance, to exclude from the selection an event composed of two fragments (^{24}Mg and $^{12}\text{C}^*$) and one α -particle finally producing one single fragment (^{24}Mg) and four α -particles. Multi-particle correlation functions [25,26] were used to identify unbound states α -particle emitters and to exclude a small percentage of events (1.6%–3.9%).

(III) It must be verified that the fragments associated with M_α are not the evaporation residues of excited Ca projectiles that have emitted sequentially α -particles only.

As far as the two first items are concerned, the effect was to suppress from 8.5% to 12.8% of previously selected events; more details can be found in Ref. [15]. The last item will be discussed in the following section.

3. Experimental Results

3.1. Evidence for Alpha-Particle Clustering

Before discussing different possible de-excitation mechanisms involved in the retained events, information on the projectile fragmentation mechanism is needed. Global features of PF events are reproduced by a model of stochastic transfers [27]. The main characteristics for primary events with $Z_{tot} = 20$ are the following: (i) excitation energy extends up to about 200 MeV, which allows the large excitation energy domain (20–150 MeV) measured for $N\alpha$ sources when associated to a single fragment (see Figure 1); (ii) angular momenta extend up to $24 \hbar$, which gives an upper spin limit for Ca projectiles or $N\alpha$ sources. We recall that excitation energies of $N\alpha$ sources are equal to the sum of kinetic energies of particles in the $N\alpha$ reference frame plus the reaction Q value.

Are α -particles emitted sequentially or simultaneously? To answer the question, α -energy spectra have been compared to simulations. For excited Ca projectiles and $N\alpha$ sources, experimental velocity and excitation energy distributions as well as distributions for spins were used as inputs. The results of the simulations were then filtered using a software replica of the multi-detector including all detection and identification details. The simulated spectra are normalized to the area of the experimental spectra. For sequential emission, the GEMINI++ code [28] was used.

Before discussing decays of $N\alpha$ sources, the possible evaporation from Ca projectiles, as stated previously, was considered. Excitation energy for projectiles is deduced from $E^* = E^*(N\alpha) + E_{rel} + Q$. E_{rel} is the relative energy between the $N\alpha$ source and the associated fragment (evaporation residue). An example of the comparison between simulation and experimental energy spectra of α -particles is displayed in Figure 2; see also Figure 6 of Ref. [15] for $N\alpha$ 4 and 6. They show a rather poor agreement, indicating that the hypothesis of sequential evaporation of alpha particles is not correct. Note that no more ^{24}Mg , ^{20}Ne or ^{16}O evaporation residues associated to $N\alpha$ from 4 to 7 are produced in simulations for ^{40}Ca spin distributions centered at values larger than $25\hbar$.

Now, considering sequential de-excitation of $N\alpha$ sources, it appears, as shown in Figure 5 of Ref. [15], that the agreement between data and simulations becomes poorer and poorer when $N\alpha$ value decreases. Moreover, an important disagreement between data and simulations is observed for the percentages of $N\alpha$ sources that de-excite via 8Be emission [15].

For simultaneous emission from $N\alpha$ sources, a dedicated simulation was made that mimics a situation in which α clusters are formed early on while the $N\alpha$ source is expanding [8,9] due to thermal pressure. By respecting the experimental excitation energy distributions of $N\alpha$ sources shown in Figure 1, a distribution of $N\alpha$ events is generated as the starting point of the simulation. Event by event, the $N\alpha$ source is first split into α 's. Then, the remaining available energy ($E^* + Q$) is directly randomly shared among the α -particles to conserve energy and linear momentum [29]. As an example, the histogram in Figure 3 is the result of such a simulation for $N\alpha = 5$ ($^{20}Ne^*$), which shows a good agreement with data; see also Figure 5 of Ref. [15] and Figure 2 of Ref. [16] for $N\alpha = 4, 6$, and 7. Similar calculated energy spectra were also obtained with simulations containing an intermediate freeze-out volume stage, where α -particles are formed and then propagated in their mutual Coulomb field. This type of simulation is used to derive density information from freeze-out volumes (see next subsection). Note that 8Be emission is out of the scope of the present simulations.

From these comparisons between both sequential and simultaneous decay simulations, it clearly appeared that sequential emission was not able to reproduce experimental data,

whereas a remarkable agreement is obtained when an α -clustering scenario is assumed. However, one cannot exclude that a few percent of $N\alpha$ sources, those produced with lower excitation energies, sequentially de-excite.

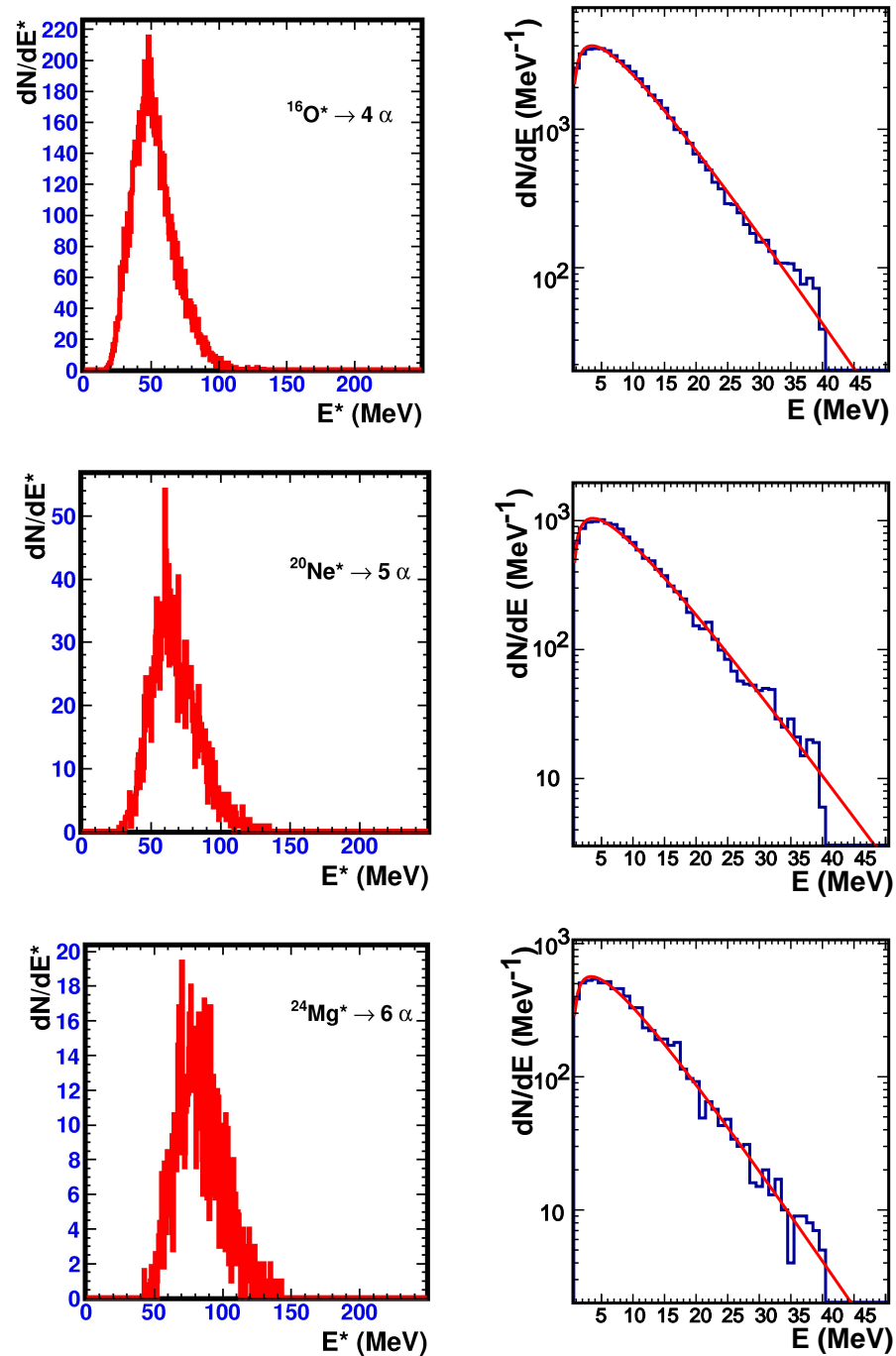


Figure 1. Cont.

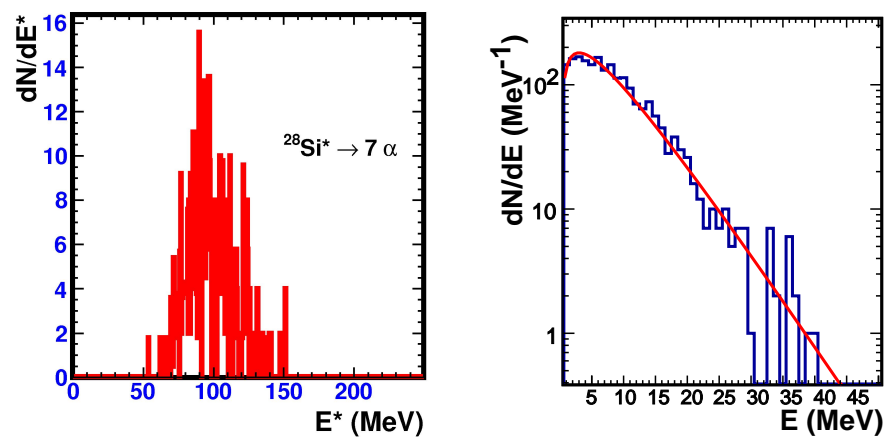


Figure 1. Excitation energy distributions (left-hand side) and α -particle energy spectra (right-hand side) for self-conjugate nuclei, from ^{16}O to ^{28}Si . Full curves superimposed on energy spectra are the results of Maxwellian fits (see text).

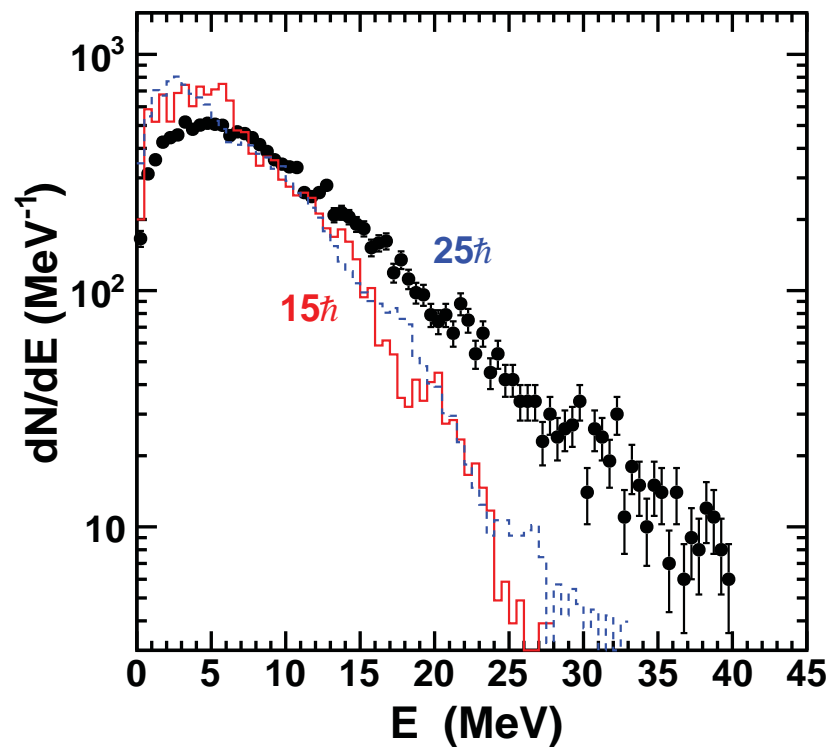


Figure 2. The sequential decay of excited Ca projectiles: energy spectra (in the $N\alpha = 5$ system reference frame) of evaporated α -particles associated to a ^{20}Ne evaporation residue. Full points are experimental data, and histograms are results of GEMINI simulations (see text). From Ref. [17].

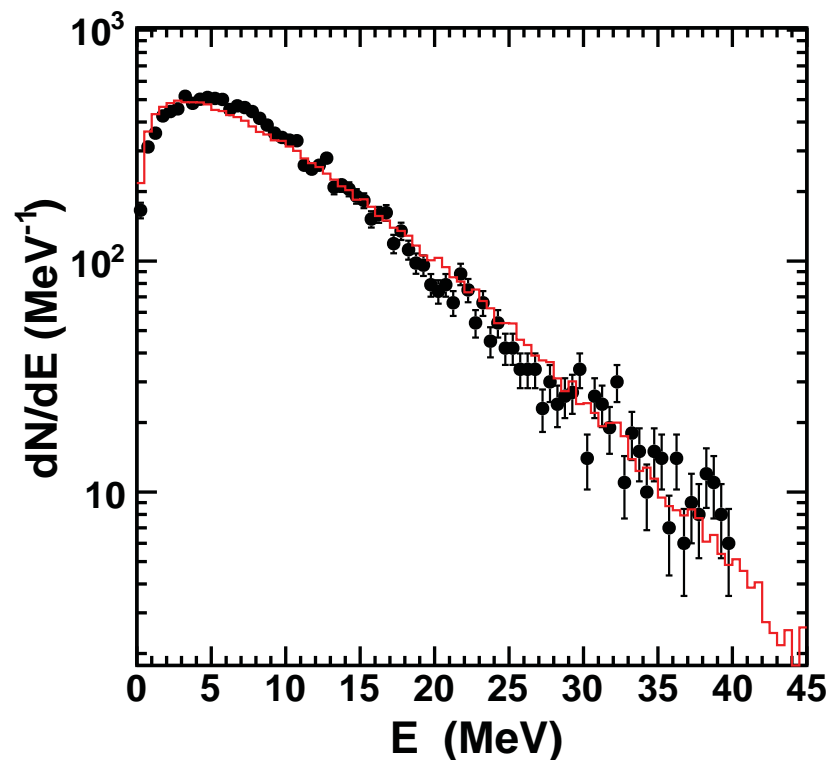


Figure 3. The alpha-particle spectrum from the $N\alpha = 5$ system ($^{20}\text{Ne}^*$). Black dots with statistical error bars correspond to experimental data (same as in Figure 2). The histogram superimposed on data corresponds to a filtered simulation of a simultaneous decay process (see text). From Ref. [17].

3.2. Alpha Clustering: Temperature and Density Information

Heavy-ion reactions at energies around the Fermi energy have been shown as good tools to create expanding nuclei and, more generally, low density nuclear matter. It is why, in the past years, various methods were used or developed to measure temperature and density in such a nuclear matter [11,14,30,31]. As we will see in what follows, we are, in our study, in a simple case to extract temperature and density information.

The excitation energy distributions of selected excited self-conjugate nuclei ($N\alpha$ sources) and the corresponding kinetic energy spectra in their reference frame are displayed in Figure 1. Excitation energy thresholds for total de-excitation into α -particles vary from 20 to 60 MeV when $N\alpha$ moves from 4 to 7, whereas the mean excitation energy per nucleon is rather constant around 3.3–3.5 MeV. Note that for the excitation spectrum of $^{28}\text{Si}^*$, even if the statistics are limited, two peaks around 110 and 125 MeV could be present, which were also observed in Ref. [32] and possibly related to toroidal high-spin isomers. Kinetic energy spectra exhibit a thermal Maxwellian shape. We recall that events with emitted pre-equilibrium α -particles were removed in our event selection (see Figure 3 of Ref. [15]), which explains our kinetic energy limit of 40 MeV.

From these spectra, temperature, T , and the Coulomb correction, C_c , are extracted from a fit procedure using a thermal Maxwellian formula:

$$dN/dE \propto (E - C_c)^{1/2} \exp[-(E - C_c)/T],$$

with a volume pre-exponential factor, which is used for the simultaneous break-up, such as alpha clustering [33]. The curves in Figure 1 correspond to Maxwellian fits, and Table 1 summarizes all the results with statistical error bars. Temperatures in the range of 5.3–6.3 MeV are extracted. C_c values that are deduced are low, around 0.3–0.5 MeV, which qualitatively indicates rather low densities for expanding excited nuclei at freeze-out due to thermal pressure. Note that with a surface pre-exponential factor $(E - B_c)$, which is used for

sequential emissions, the best fits to the same data are of lower quality and can only be achieved by allowing negative values for the Coulomb barrier B_c . Such negative values have no physical meaning, and the necessity to use a volume pre-exponential factor further confirms the simultaneous emission of α -particles, which characterizes the clustering.

Table 1. Alpha-clustering for self-conjugate nuclei. Excitation energy information: the mean value $\langle E^* \rangle$ and standard deviation σ_{E^*} . Parameters from Maxwellian fits to energy spectra: temperature T and Coulomb correction C_c . Densities normalized to saturation density ρ_0 have been deduced from simulations (see text). Statistical errors are within parentheses.

Nucleus	$\langle E^* \rangle$ (MeV)	σ_{E^*} (MeV)	T (MeV)	C_c (MeV)	ρ/ρ_0
^{16}O	52.4	15.7	6.15 (0.03)	0.33 (0.03)	0.37 (0.04)
^{20}Ne	67.3	16.7	6.22 (0.05)	0.45 (0.05)	0.36 (0.04)
^{24}Mg	83.5	17.4	5.92 (0.07)	0.40 (0.07)	0.34 (0.06)
^{28}Si	98.5	17.6	5.40 (0.12)	0.37 (0.16)	0.34 (0.11)

To derive quantitative density information, the Coulomb corrections parameters deduced from the fits, C_c , have been used. As mentioned in the previous subsection, dedicated simulations were made to be compared with kinetic energy spectra. By imposing temperatures deduced from the fits (see Table 1) within a simulation containing an intermediate freeze-out volume stage, it was easy to determine freeze-out volumes by also imposing an agreement with the most probable value of kinetic energy spectra, which is equal to $T/2 + C_c$. Freeze-out volumes values are in the range $2.7\text{--}3.0V_0$, V_0 being the volumes of self-conjugate nuclei at the saturation density. The corresponding normalized densities ρ/ρ_0 are indicated in Table 1.

4. Discussion

As mentioned in the introduction, two self-consistent mean field calculations have been performed by imposing constrained deformation with a restriction to spherical symmetric configurations [8,9]. By gradually increasing the nuclear radius, the density of self-conjugate nuclei is decreased, and at a certain density value, the formation of clusters appears. The first calculation was made with the constrained Hartree–Fock–Bogoliubov approach using the Gogny D1S interaction, and in the second, the self-consistent relativistic Hartree–Bogoliubov model with the effective interaction DD-ME2 has been employed. For a comparison of the density needed for α -clustering, one can refer in the calculations to the clustering radius normalized to the ground state radius $r_c/r_{g.s.}$. In the first simulation, this ratio is found around 1.8 for ^{16}O and ^{24}Mg , whereas in the second, a smaller value around 1.3 is obtained for ^{16}O . The explanation given in Ref. [9] is the fact that the single-nucleon localization is more pronounced with the relativistic functional, which facilitates the formation of α clusters in excited states. Directly translated into densities, these ratios correspond to ρ/ρ_0 around 0.17 [8] and 0.45 [9]. However, it is important to stress that calculations contain their own spurious center of mass energy, which should be removed. In Ref. [8], an estimate of the correction needed was made starting from a calculation performed on ^8Be , constraining the distance between the two nascent α -particles. About 14 MeV were found to be missing to get twice the binding energy of a single particle in the asymptotic limit. Thus, a correction of 7 MeV per α -particle was made, whatever the self-conjugate nucleus (from ^{16}O to ^{28}Si) and as a consequence the density for the appearance of α -clustering was increased to $\rho/\rho_0 \sim 1/3$, which is close to our results. However, regarding these calculations, an important point one must underline is the fact that they correspond to zero temperature.

In Ref. [7], a generalized relativistic mean field model is used to calculate α -particle fractions in symmetric matter at subsaturation density for different temperatures. In particular, this work describes the sudden decrease of the α -particle fraction at high densities by the vanishing of α -particle binding energy due to the Pauli blocking that leads to the

Mott effect, i.e., the dissolution of α -particles in the medium. Thus, the maximum cluster abundance is reached around the Mott density. At a temperature of 6 MeV, this density is also $\sim \rho_0/3$.

To conclude, we can say that α -clustering in self-conjugate nuclei, experimentally deduced from ^{16}O to ^{28}Si , occurs around $T = 5.5\text{--}6.0$ MeV and densities in the range of $\rho/\rho_0 = 0.3\text{--}0.4$. At present, the constrained self consistent mean field calculations at zero temperature are in qualitative agreement for densities, but even more realistic calculations are needed for a valuable comparison with data.

Author Contributions: Writing original draft, review and editing, B.B., methodology, B.B.; formal analysis, B.B. and A.R.; software acquisition, E.D.F. and G.C.; data reduction, E.D.F., E.G., N.L.N. and A.R.; detectors and hardware, G.L., I.L., O.L., C.M., A.P., M.P., S.P., F.R. and P.R. All authors have read and agreed to the published version of the manuscript.

Funding: This research was supported by INFN and IN2P3/CNRS.

Institutional Review Board Statement: Not applicable.

Informed Consent Statement: Not applicable.

Data Availability Statement: Not applicable.

Conflicts of Interest: The authors declare no conflict of interest.

References

1. Fischer, T.; Hempel, M.; Sagert, I.; Suwa, Y.; Schaffner-Bielich, J. Symmetry energy impact in simulations of core-collapse supernovae. *Eur. Phys. J. A* **2014**, *50*, 46. [\[CrossRef\]](#)
2. Arcones, A.; Martínez-Pinedo, G.; O'Connor, E.; Schwenk, A.; Janka, H.T.; Horowitz, C.J.; Langanke, K. Influence of light nuclei on neutrino-driven supernova outflows. *Phys. Rev. C* **2008**, *78*, 015806. [\[CrossRef\]](#)
3. Röpke, G.; Schnell, A.; Schuck, P.; Noziers, P. Four-Particle Condensate in Strongly Coupled Fermion systems. *Phys. Rev. Lett.* **1998**, *80*, 3177–3180. [\[CrossRef\]](#)
4. Beyer, M.; Sofianos, S.A.; Kuhrts, C.; Röpke, G.; Schuck, P. The α -particle in nuclear matter. *Phys. Lett. B* **2000**, *488*, 247–253. [\[CrossRef\]](#)
5. Horowitz, C.J.; Schwenk, A. Cluster formation and the virial equation of state of low-density nuclear matter. *Nucl. Phys. A* **2006**, *776*, 55–79. [\[CrossRef\]](#)
6. Samadar, S.K.; De, J.N.; Viñas, X.; Centelles, M. Symmetry coefficients and incompressibility of clusterized supernova matter. *Phys. Rev. C* **2009**, *80*, 035803. [\[CrossRef\]](#)
7. Typel, S.; Röpke, G.; Klähn, T.; Blaschke, D.; Wolter, H.H. Composition and thermodynamics of nuclear matter with light clusters. *Phys. Rev. C* **2010**, *81*, 015803. [\[CrossRef\]](#)
8. Girod, M.; Schuck, P. α -Particle Clustering from Expanding Self-Conjugate Nuclei within the Hartree-Fock-Bogoliubov Approach. *Phys. Rev. Lett.* **2013**, *111*, 132503. [\[CrossRef\]](#) [\[PubMed\]](#)
9. Ebran, J.-P.; Khan, E.; Nikšić, T.; Vretenar, D. Cluster-liquid transition in finite, saturated fermionic systems. *Phys. Rev. C* **2014**, *89*, 031303(R). [\[CrossRef\]](#)
10. Ebran, J.-P.; Girod, M.; Khan, E.; Lasserri, R.D.; Schuck, P. α -particle condensation: A nuclear quantum phase transition. *Phys. Rev. C* **2020**, *102*, 014305. [\[CrossRef\]](#)
11. Qin, L.; Hagel, K.; Wada, R.; Natowitz, J.B.; Shlomo, S.; Bonasera, A.; Röpke, G.; Typel, S.; Chen, Z.; Huang, M.; et al. Laboratory Tests of Low Density Astrophysical Nuclear Equation of State. *Phys. Rev. Lett.* **2012**, *108*, 172701. [\[CrossRef\]](#)
12. Hempel, M.; Hagel, K.; Natowitz, J.; Röpke, G.; Typel, S. Constraining supernova equation of state with equilibrium constants from heavy-ion collisions. *Phys. Rev. C* **2015**, *91*, 045805. [\[CrossRef\]](#)
13. Pais, H.; Bougault, R.; Gulminelli, F.; Providência, C.; Bonnet, E.; Borderie, B.; Chbihi, A.; Frankland, J.D.; Galichet, E.; Gruyer, D.; et al. Low Density In-Medium Effects on Light Clusters from Heavy-Ion Data. *Phys. Rev. Lett.* **2020**, *125*, 012701. [\[CrossRef\]](#)
14. Pais, H.; Bougault, R.; Gulminelli, F.; Providência, C.; Bonnet, E.; Borderie, B.; Chbihi, A.; Frankland, J.D.; Galichet, E.; Gruyer, D.; et al. Improved method for the experimental determination of in-medium effects from heavy-ion collisions. *J. Phys. G Nucl. Part. Phys.* **2020**, *47*, 105204. [\[CrossRef\]](#)
15. Borderie, B.; Raduta, A.R.; Ademard, G.; Rivet, M.F.; De Filippo, E.; Geraci, E.; Le Neindre, N.; Alba, R.; Amorini, F.; Cardella, G.; et al. Probing clustering in excited alpha-conjugate nuclei. *Phys. Lett. B* **2016**, *755*, 475–480. [\[CrossRef\]](#)
16. Borderie, B.; Raduta, A.R.; Ademard, G.; Rivet, M.F.; De Filippo, E.; Geraci, E.; Le Neindre, N.; Alba, R.; Amorini, F.; Cardella, G.; et al. Alpha-particle clustering in excited alpha-conjugate nuclei. *J. Phys. Conf. Ser.* **2017**, *863*, 012054. [\[CrossRef\]](#)
17. Borderie, B.; Raduta, A.R.; Ademard, G.; Rivet, M.F.; De Filippo, E.; Geraci, E.; Le Neindre, N.; Cardella, G.; Lanzalone, G.; Lombardo, I.; et al. Alpha-particle clustering in excited expanding self-conjugate nuclei. *EPJ Web. Conf.* **2016**, *117*, 07014. [\[CrossRef\]](#)

18. Borderie, B.; Rivet, M.F.; Tassan-Got, L. Heavy-ion peripheral collisions in the Fermi energy domain—Fragmentation processes or dissipative collisions. *Ann. Phys. Fr.* **1990**, *15*, 287–390. [\[CrossRef\]](#)
19. Morjean, M.; Charvet, J.L.; Uzureau, J.L.; Patin, Y.; Peghaire, A.; Pranal, Y.; Sinopoli, L.; Billerey, A.; Chevarier, A.; Chevarier, N.; et al. Nuclear fragmentation processes in the $^{20}\text{Ne} + ^{27}\text{Al}$ system at 30 MeV/A. *Nucl. Phys. A* **1985**, *438*, 547–563. [\[CrossRef\]](#)
20. Pagano, A.; Alderighi, M.; Amorini, F.; Anzalone, A.; Arena, L.; Auditore, L.; Baran, V.; Bartolucci, M.; Berceanu, I.; Blicharska, J.; et al. Fragmentation studies with the CHIMERA detector at LNS in Catania: Recent progress. *Nucl. Phys. A* **2004**, *734*, 504–511. [\[CrossRef\]](#)
21. Alderighi, M.; Anzalone, A.; Bassini, R.; Berceanu, I.; Blicharska, J.; Boiano, C.; Borderie, B.; Bougault, R.; Bruno, M.; Calí, C.; et al. Particle identification method in the CsI(Tl) scintillator used for the CHIMERA 4pi detector. *Nucl. Instr. Meth. Phys. Res. A* **2002**, *489*, 257–265. [\[CrossRef\]](#)
22. Le Neindre, N.; Alderighi, M.; Anzalone, A.; Barnà, R.; Bartolucci, M.; Berceanu, I.; Borderie, B.; Bougault, R.; Bruno, M.; Cardella, G.; et al. Mass and Charge identification of fragments detected with the Chimera Silicon-CsI(Tl) telescopes. *Nucl. Instr. Meth. Phys. Res. A* **2002**, *490*, 251–262. [\[CrossRef\]](#)
23. Eudes, P.; Basrak, Z.; Sébille, F.; De la Mota, V.; Royer, G. Comprehensive analysis of fusion data well above the barrier. *Phys. Rev. C* **2014**, *90*, 034609. [\[CrossRef\]](#)
24. Fuchs, H.L.; Moring, K. Heavy-ion break-up processes in the Fermi energy range. *Rep. Prog. Phys.* **1994**, *57*, 231–324. [\[CrossRef\]](#)
25. Charity, R.J.; Sobotka, L.G.; Robertson, N.J.; Sarantites, D.G.; Dinius, J.; Gelbke, C.K.; Glasmacher, T.; Handzy, D.O.; Hsi, W.C.; Huang, M.J.J.; et al. Prompt and sequential decay processes in the fragmentation of 40 MeV/nucleon ^{20}Ne projectiles. *Phys. Rev. C* **1995**, *52*, 3126–3150. [\[CrossRef\]](#) [\[PubMed\]](#)
26. Lisa, M.A.; Gong, W.G.; Gelbke, C.K.; Lynch, W.G. Event-mixing analysis of two-proton correlation functions. *Phys. Rev. C* **1991**, *44*, 2865–2868. [\[CrossRef\]](#)
27. Tassan-Got, L.; Stephan, C. Deep inelastic transfers: A way to dissipate energy and angular momentum for reactions in the Fermi energy domain. *Nucl. Phys. A* **1991**, *524*, 121–140. [\[CrossRef\]](#)
28. Charity, R.J. Systematic description of evaporation spectra for light and heavy compound nuclei. *Phys. Rev. C* **2010**, *82*, 014610. [\[CrossRef\]](#)
29. Lopez, A.; Randrup, J. Multifragmentation versus sequential fission: Observable differences? *Nucl. Phys. A* **1989**, *491*, 477–491. [\[CrossRef\]](#)
30. Marini, P.; Zheng, H.; Boisjoli, M.; Verde, G.; Chbihi, A.; Napolitani, P.; Ademard, G.; Augey, L.; Bhattacharya, C.; Borderie, B.; et al. Signals of Bose Einstein condensation and Fermi quenching in the decay of hot nuclear systems. *Phys. Lett. B* **2016**, *756*, 194–199. [\[CrossRef\]](#)
31. Mabilia, J.; Zheng, H.; Bonasera, A.; Kohley, Z.; Yennello, S.J. Competition between fermions and bosons in nuclear matter at low densities and finite temperatures. *Phys. Rev. C* **2016**, *94*, 064617. [\[CrossRef\]](#)
32. Cao, X.G.; Kim, E.J.; Schmidt, K.; Hagel, K.; Barbui, M.; Gauthier, J.; Wuenschel, S.; Giuliani, G.; Rodriguez, M.R.D.; Kowalski, S.; et al. Examination of evidence for resonances at high excitation energy in the 7α disassembly of ^{28}Si . *Phys. Rev. C* **2019**, *99*, 014606. [\[CrossRef\]](#)
33. Goldhaber, A. Volume versus surface sampling of Maxwellian distributions in nuclear reactions. *Phys. Rev. C* **1978**, *17*, 2243–2244. [\[CrossRef\]](#)